DOI: 10.1002/ejic.200801203

Hydrothermal Synthesis of Monodisperse $Ce_{0.5}Zr_{0.5}O_2$ Metastable Solid Solution Nanocrystals

Takaaki Taniguchi,*[a] Tomoaki Watanabe,[b] Nobuhiro Matsushita,[a] and Masahiro Yoshimura[a]

Keywords: Nanostructures / Hydrothermal synthesis / Solid solutions / Heterogeneous catalysis

An environmentally friendly and economically efficient method has been developed to synthesize monodisperse CeO_2-ZrO_2 solid solution nanocrystals. In this process, the formation of oleate-stabilized $Ce_{0.5}Zr_{0.5}O_2$ nanocrystals was designed to proceed through hydrolytic sol–gel condensation of metal–oleate precursors in an aqueous solution and subsequent hydrothermal growth at 200 °C for 6 h. The results showed that the 3.0-nm-sized nanocrystals possess a metastable CeO_2-ZrO_2 tetragonal phase with well-designed chemical composition and are nearly monodisperse. Owing to the uniform textural and elemental properties, the products exhibit relatively high thermal stability of the metastable phase and well-defined reduction properties.

Introduction

Doping a metal oxide with a heterometallic ion has a strong impact on its physical and chemical properties and results in the enhancement or generation of material functions. Therefore, the design of solid solution nanostructures is essential in the search of advanced nanomaterials. Investigation of CeO_2-ZrO_2 binary catalysts demonstrates this research direction. A simple oxide, CeO_2, shows redox properties due to the reversible oxidation/reduction of $Ce^{4+} \leftrightarrow Ce^{3+}$, which offers properties suitable for an efficient three-way catalyst (TWC) for treating exhaust gas from automobiles and a water-gas-shift (WGS) catalyst to produce H_2 fuel.[1] Furthermore, doping CeO_2 with an additional oxide, MO_x (M = Re, Cu, Mn, Bi, Zr, etc), often enhances the catalytic activity, as a result of the improvement in the redox properties as well as in the thermal stability of the nanostructures.[2] Among various binary systems, the CeO_2-ZrO_2 system, or doping with ZrO_2, is considered to beneficially enhance the catalytic properties of CeO_2, and, in fact, much research has already been performed on the synthesis and analysis of nanostructured CeO_2-ZrO_2 solid solutions, as reviewed by Monte and Kaspar.[3]

Even though continuous efforts have enabled the synthesis of unique nanostructures based on CeO_2-ZrO_2, such as ordered mesoporous structures and nanocages of the solid solution,[4] monodisperse CeO_2-ZrO_2 nanoparticles, which should be important for the fabrication of nanostructured catalysts by the bottom-up approach based on nanoparticle assembly, have not been available so far. This is probably because conventional approaches provide limited control over the chemical composition, crystalline phase, and particle size of the resultant nanoparticles. For example, aqueous approaches based on a precipitation method normally produce aggregates of CeO_2-ZrO_2 nanocrystals without redispersibility in any solvent, although it is possible to tailor the chemical composition of the solid solution.[5] In addition, nonaqueous routes, such as thermal decomposition of a metal–surfactant complex, are effective for preparing monodisperse nanoparticles consisting of a single metal component oxide, including CeO_2[6] and ZrO_2.[7] However, the lack of a process controlling the reactivity of the heterometallic reactants in these approaches clearly makes it difficult to use them for the synthesis of solid solution oxides; in fact, the thermal decomposition method has resulted in the production of agglomerated and poorly crystalline CeO_2-ZrO_2 nanoparticles.[8]

To overcome the drawbacks of conventional methods, an oleate-aided hydrothermal approach has been developed. By using this approach, nearly monodisperse nanocrystals based on $EuO_{1.5}$-doped HfO_2 and $GdO_{1.5}$-doped CeO_2 having dopant concentrations of less than 20 mol-%, have been successfully synthesized by an oleate-modified nucleation-hydrothermal growth process.[9] Furthermore, utilization of inexpensive and less toxic aqueous solutions during all the synthetic steps throughout the process provides the possible application of the proposed method in industry.

In the present study, this attractive approach has been employed for the synthesis of CeO_2-ZrO_2 solid solution nanoparticles with an atomic Ce/Zr ratio of unity. In order

[a] Materials and Structures Laboratory, Tokyo Institute of Technology,
4259 Midori, Nagatsuta, Yokohama 226-8503, Japan
Fax: +81-45-924-5358
E-mail: taka.tani@msl.titech.ac.jp
[b] Department of Applied Chemistry, Meiji University,
1-1-1 Higashimita, Tama-ku, Kawasaki 214-8571, Japan

to characterize the CeO_2-ZrO_2 nanocrystals formed, their structural, elemental, morphological, and catalytic properties were investigated by energy dispersive X-ray (EDX), XRD, and Raman spectroscopy, as well as by the transmission electron microscopy (TEM) and temperature-programmed reduction (TPR) techniques.

Results and Discussion

The formation of $Ce_{0.5}Zr_{0.5}O_2$ nanocrystals was designed to proceed through a hydrolytic condensation of Ce/Zr–oleate complex by base and subsequent hydrothermal growth. Following the reaction mechanism suggested in our earlier works,[9] this process can simultaneously perform the coprecipitation of Ce and Zr cations to form the solid solution framework and also allow oleate surface modification of hydrothermally grown nanocrystals by in situ oleate stabilization through the processes of condensation, nucleation, and crystal growth. The overview of the reaction pathway was confirmed by testing the colloidal stability and performing elemental analysis by using EDX spectroscopy. First, the products could readily be dispersed in cyclohexane to form a yellowish transparent colloidal solution, which showed the hydrophobic nature of nanocrystals passivated by the fatty acid. Subsequently, the atomic Ce/Zr ratio of 54:46, obtained by EDX analysis, corresponded well to that of the initial materials. These preliminary results indicate that the reaction to produce the fatty-acid-passivated CeO_2-ZrO_2 nanocrystals was followed as designed.

Figure 1a shows XRD patterns of as-prepared $Ce_{0.5}Zr_{0.5}O_2$ nanoparticles, as well as a reference sample of undoped CeO_2 nanoparticles. The pattern of the $Ce_{0.5}Zr_{0.5}O_2$ sample corresponded to the cubic CeO_2 phase (JCPDS. No. 34–0394) and showed no reflections from a monoclinic ZrO_2 phase. The average crystallite size of the $Ce_{0.5}Zr_{0.5}O_2$, calculated by the Debye–Scherrer formula, was 3.0 nm, which was smaller than that of CeO_2 nanocrystals (5.2 nm). The decrease in crystallite size, due to the incorporation of ZrO_2 with CeO_2, has commonly been reported in the wet chemical syntheses of this binary oxide.[5,10] Indeed, peaks of the XRD pattern for the CeO_2-ZrO_2 sample slightly shifted to higher angles compared to those for the undoped CeO_2 sample, indicating a smaller *d*-spacing in the CeO_2-ZrO_2 nanocrystals than in the CeO_2 nanocrystals. Since the ionic radius of Zr^{4+} in an octahedral environment (0.84 Å) is smaller than that of Ce^{4+} (0.97 Å), the atomic-scale incorporation of ZrO_2 in the CeO_2 matrix could result in these *d*-spacing changes. Accordingly, the crystalline size/phase evaluations by XRD strongly indicate the formation of a solid solution rather than physical mixtures of CeO_2-and ZrO_2-based compounds; however, this analysis is not sufficient to determine the crystalline phase of CeO_2-ZrO_2 nanoparticles. Although the cubic and tetragonal phase can be formed in a metastable state, broadening of reflections due to the small grains prevents detection of considerable tetragonal distortion, such as splitting of the (400) and (004) reflections. Raman spectroscopy was employed to identify the crystalline phase of hydrothermally synthesized $Ce_{0.5}Zr_{0.5}O_2$ nanoparticles. According to the selection rules, the tetragonal phase ($P4_2/nmc$) has six ($1A_g + 2B_g + 3E_g$) Raman-active modes, whereas the cubic phase ($Fm3m$) has one Raman active mode (F_{2g}). Thus, the Raman band features are indicators that distinguish between the cubic and tetragonal phases of the solid solution.[11] Figure 1b shows the Raman spectra of CeO_2 and $Ce_{0.5}Zr_{0.5}O_2$ nanocrystals prepared by hydrothermal methods. As can be seen in this figure, undoped CeO_2 nanoparticles show a sharp and intense peak at 460 cm^{-1}, corresponding to the F_{2g} mode of the cubic phase, while the spectrum of $Ce_{0.5}Zr_{0.5}O_2$ nanoparticles exhibits several bands, at 132, 311, 475, and 642 cm^{-1}. The band features involving band numbers, peak positions, and overall shapes of the latter spectrum closely resemble the characteristics of the Raman spectrum previously assigned to the tetragonal CeO_2-ZrO_2 phase,[11] which suggests that the metastable tetragonal form is a predominant phase of the products.

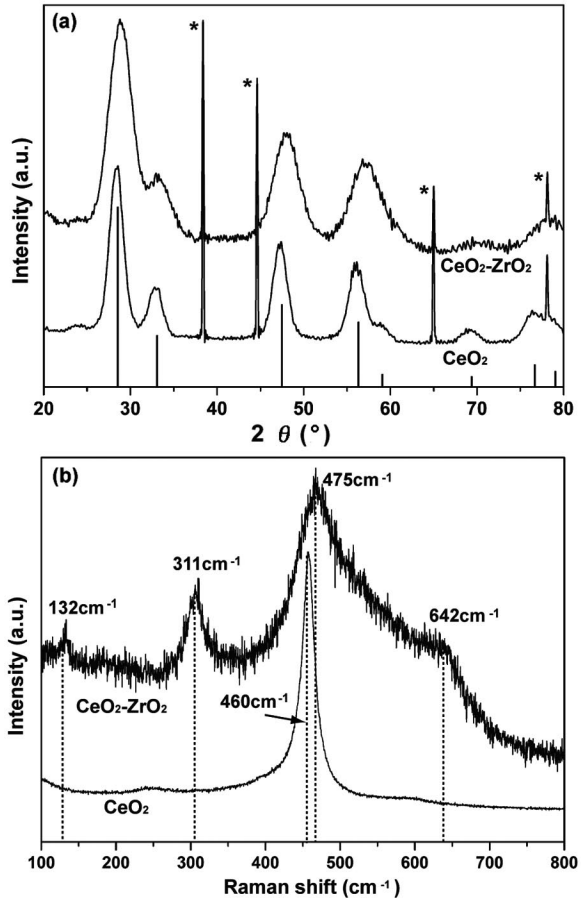

Figure 1. (a) X-ray powder diffraction patterns and (b) Raman spectra of CeO_2 and $Ce_{0.5}Zr_{0.5}O_2$ nanoparticles synthesized by hydrothermal methods at 200 °C for 6 h. In Figure 1a, vertical lines corresponding to cubic fluorite CeO_2 (JCPDS No. 34–104) are shown for comparison, and peaks of an internal standard, Al (cubic, a = 4.0494 Å), are indicated by asterisks.

Individual nanoparticles were analyzed by TEM. Figure 2a shows a low-magnification TEM image of $Ce_{0.5}Zr_{0.5}O_2$ nanoparticles synthesized by the hydrothermal method. As expected from the high colloidal stability, the observed nanoparticles were highly dispersed without any tendency to agglomerate. Moreover, the spherically shaped particles had a rather uniform size. According to the TEM analysis, the average size of the nanoparticles was 3.3 nm. Since this is very close to the crystallite size obtained by XRD analysis (3.0 nm), each nanoparticle should be a monocrystal. This possibility was confirmed by a subsequent high-resolution TEM analysis. As shown in Figure 2b, a representative nanoparticle has no grain boundaries, clearly indicating its single-crystalline nature. Moreover, the particle is considered to be highly crystallized, since no lattice dislocation, secondary phase, or amorphous surface layer was seen.

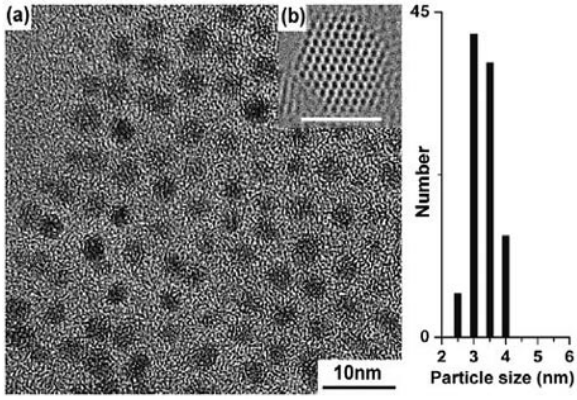

Figure 2. TEM images of $Ce_{0.5}Zr_{0.5}O_2$ nanoparticles prepared by the hydrothermal method: (a) a low-magnification TEM image and (b) a HRTEM image of an isolated nanocrystal (the scale bar corresponds to 4 nm).

Samples calcined in air were investigated further by XRD analysis. Monitoring the thermally induced phase degradation of the metastable CeO_2-ZrO_2 phase by XRD is useful for analyzing the local domain structure. A homogeneous distribution of the Ce and Zr cations in the lattice slows the process of phase segregation, while the ZrO_2- or CeO_2-rich nanodomains act as nuclei for the segregation, thus speeding up the kinetics of the process.[3] Figure 3a shows the XRD patterns of $Ce_{0.5}Zr_{0.5}O_2$ samples annealed at 900 and 1000 °C for 5 h. No remarkable phase degradation was observed after calcination at 900 °C, whereas reflections became sharper as a result of grain growth in the calcination process. Phase separation was clearly observed after calcination at 1000 °C; the (111) reflection detected at a 2θ value of ca. 29° in the pattern of the sample calcined at 900 °C separated to lower and higher angles (see Figure 3b). These separated phases might correspond to cubic and tetragonal phases containing approximately 95 and 2.5 mol-% CeO_2, respectively, based on the solubility limits of CeO_2 and ZrO_2 at 1000 °C.[5,11] It is also notable that any reflections from a monoclinic ZrO_2 phase were not detectable. The calcination temperature of 1000 °C, producing significant degradation of the metastable form, is comparable to previously reported data. For example, $Ce_{0.5}Zr_{0.5}O_2$ nanocrystals prepared by citrate complexation and hydrothermal methods show degradation temperatures of 1000[10] and 1100 °C,[11] respectively. These indicate that the CeO_2-ZrO_2 nanocrystals produced by the proposed method have a quite uniform domain with an atomic Ce/Zr ratio close to unity, unlike the multiphase mixtures that widely cover x values of $Ce_{1-x}Zr_xO_2$.

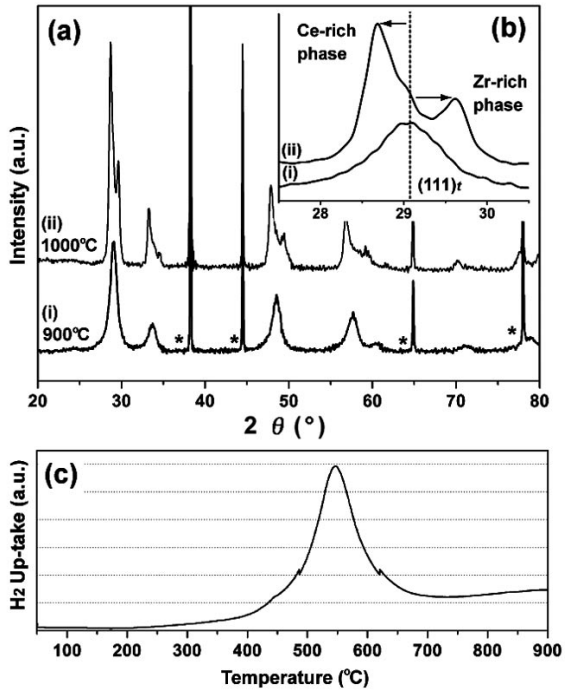

Figure 3. (a) Wide-angle and (b) selected-angle X-ray powder diffraction patterns of $Ce_{0.5}Zr_{0.5}O_2$ nanocrystals calcined at (i) 900 and (ii) 1000 °C for 5 h. Peaks of an internal standard, Al (cubic, a = 4.0494 Å), are indicated by asterisks. (c) TPR profile of $Ce_{0.5}Zr_{0.5}O_2$ nanocrystals calcined at 900 °C for 5 h.

Redox properties of the CeO_2-ZrO_2 sample were also tested by the TPR technique. Figure 3c shows the TPR profile of the $Ce_{0.5}Zr_{0.5}O_2$ sample calcined at 900 °C for 5 h. A detectable peak, centered on 547 °C, corresponds well to a characteristic reduction temperature of a CeO_2–ZrO_2 solid solution measured under similar experimental conditions (use of H_2 gas for reducing agent, the absence of loading of a noble metal support, and special pretreatment).[12] Indeed, distinct peaks related to bulk and surface reductions, which are usually observed in nanocrystalline undoped CeO_2, are not seen in the profile,[12] thus indicating an absence of remarkably CeO_2-rich domains. Therefore, the TPR analysis further supports the textural and elemental homogeneities of the solid solution nanocrystals and also presents potential uses of the hydrothermal products in catalytic applications.

Conclusions

In the present study, we have reported oleate-aided hydrothermal synthesis of $Ce_{0.5}Zr_{0.5}O_2$ nanocrystals for the

first time. EDX, XRD, and Raman spectroscopy showed that these nanocrystals have a metastable tetragonal phase with a closely designed chemical composition. TEM analysis revealed that the approximately 3.0-nm-sized nanocrystals are highly crystallized and nearly monodisperse. The relatively high thermal stability of the metastable phase and the reasonable reduction properties suggest that the nanocrystals exhibit rather uniform textural and elemental properties. Accordingly, it is demonstrated that the proposed hydrothermal approach could provide these nanocrystals with a high uniformity of morphological, physical, and chemical properties. Therefore, the products should be useful in advanced catalytic applications.

Experimental Section

Hydrothermal Synthesis: A total amount of 3.5 mmol of $(NH_4)_2Ce(NO_3)_6$ (Wako, 99.5%) and $ZrOCl_2{\cdot}8H_2O$ (Wako, 99.5%), with Zr/(Ce+Zr) = 50%, was dissolved in distilled water (15 mL) at room temperature. Then sodium oleate ($C_{17}H_{33}COONa$), (3.5 mmol, Wako, analytical grade) dissolved in distilled water (15 mL) was added to the aqueous solution containing Ce and Zr ions to form a Ce/Zr–oleate complex at room temperature under vigorous stirring. Subsequently, ammonia (5 mL, 25 wt.-% aqueous solution, Wako, analytical grade) was added to the solution mixture. Then, the reaction mixture was placed in a polytetrafluoroethylene (PTFE) vessel (inner volume: 40 cm^3). The vessel was sealed and placed inside a stainless steel autoclave, which was kept at 200 °C for 6 h under autogenous pressure. The products were collected by centrifugation (5000 rpm for 30 min), washed twice with distilled water, and then dried at 150 °C for 6 h in air. Note that Na^+ ions, which were possibly adsorbed on the surface of the products, were mostly removed in the washing process, so that no Na was detected by EDX measurements (data not shown). For comparison, an undoped CeO_2 reference sample was prepared. A single precursor of $(NH_4)_2Ce(NO_3)_6$, (3.5 mmol) was used for this synthesis. The rest of the experimental procedure was the same as that for the doped sample. $Ce_{0.5}Zr_{0.5}O_2$ samples calcined at 900 and 1000 °C for 5 h were also investigated. The treatment involved heating for 2 h up to the final temperature and isothermal annealing for 5 h.

Characterizations: The crystalline products were characterized by XRD spectroscopy with a Rigaku RINT 2000 diffractometer having Ni-filtered Cu-K_α radiation (λ = 1.54178 Å). The average crystallite sizes were calculated by the Debye–Scherrer formula, by using the line broadening of a (220) refraction of a cubic phase. TEM analyses were performed by using a Hitachi HF-2000 instrument operating at 200 kV. For TEM measurements, one drop of the sample, dispersed in cyclohexane, was deposited on an amorphous carbon grid. The average contents of cerium and zirconium were quantified by using an EDX spectrometer attached to a scanning electron microscope (Hitachi S-4500) operated at 15 kV. Raman spectroscopy was carried out with a Jobin Yvon T64000 spectrometer (resolution of 1 cm^{-1}) by using a visible laser (λ = 514.5 nm) with an output power of 50 mW at room temperature. The scattered light was collected in back-scattering geometry by using a liquid-nitrogen-cooled charge-coupled device (CCD) detector. The samples were pre-irradiated by an excitation laser for approximately 5 min to remove background photoluminescence that might be coming from organics, and then the measurements were made. TPR profiles were measured with an Ohkura Riken TP-5000 instrument. First, the sample calcined at 900 °C for 5 h was pretreated at 500 °C for 15 min, under dry air flow (30 mL/min), and then it was cooled in an Ar flow from 150 °C to room temperature to purge O_2. The TPR measurement was then made under 10%H_2/Ar flow (30 mL/min) at a constant heating ratio of 10 °C/min up to 900 °C.

Acknowledgments

We express our gratitude to Dr. A. Ahiniyaz (Ytkemiska Institutet, Institute for Surface Chemistry) and Dr. Y. V. Kolen'ko (Max Planck Institute) for fruitful discussions. We also thank K. Yokota (Anan Kasei Co. Ltd) for the TPR measurement and Dr. C. S. Kuroda (Tokyo Institute of Technology) for assistance with TEM analyses.

[1] a) A. Trovarelli, C. de Leitenburg, M. Boaro, G. Dolcetti, *Catal. Today* **1999**, *50*, 353; b) J. Kaspar, P. Fornasiero, M. Graziani, *Catal. Today* **1999**, *50*, 285; c) Q. Fu, H. Saltsburg, M. Flytzani-Stephanopoulos, *Science* **2003**, *301*, 935–938.
[2] a) B. Bonnetot, V. Rakic, T. Yuzhakova, C. Guimon, A. Auroux, *Chem. Mater.* **2008**, *20*, 1585; b) B. M. Reddy, A. Khan, *Catal. Surv. Asia* **2005**, *9*, 155; c) N. Imanaka, T. Masui, K. Koyabu, K. Minami, T. Egawa, *Adv. Mater.* **2007**, *19*, 1608; d) G. Sedmak, S. Hocevar, J. Levec, *J. Catal.* **2003**, *213*, 135; e) M. Machida, M. Uto, D. Kurogi, T. Kijima, *Chem. Mater.* **2000**, *12*, 3158.
[3] R. Di Monte, J. Kaspar, *J. Mater. Chem.* **2005**, *15*, 633.
[4] a) Q. Yuan, Q. Liu, W. G. Song, W. Feng, W. L. Pu, L. D. Sun, Y. W. Zhang, C. H. Yan, *J. Am. Chem. Soc.* **2007**, *129*, 6698; b) A. Corma, P. Atienzar, H. Garcia, J. Y. Chane-Ching, *Nat. Mater.* **2004**, *3*, 394; c) T. Brezesinski, M. Antonietti, M. Groenewolt, N. Pinna, B. Smarsly, *New J. Chem.* **2005**, *29*, 237; d) X. Liang, X. Wang, Y. Zhuang, B. Xu, S. M. Kuang, Y. D. Li, *J. Am. Chem. Soc.* **2008**, *130*, 2736.
[5] a) A. Ahniyaz, T. Fujiwara, T. Fujino, M. Yoshimura, *J. Nanosci. Nanotechnol.* **2004**, *4*, 233; b) A. S. Deshpande, N. Pinna, P. Beato, M. Antonietti, M. Niederberger, *Chem. Mater.* **2004**, *16*, 2599.
[6] a) S. W. Yang, L. Gao, *J. Am. Chem. Soc.* **2006**, *128*, 9330; b) T. Y. Yu, J. Joo, Y. I. Park, T. Hyeon, *Angew. Chem. Int. Ed.* **2005**, *44*, 7411; c) H. Gu, M. D. Soucek, *Chem. Mater.* **2007**, *19*, 1103.
[7] a) J. Joo, T. Yu, Y. W. Kim, H. M. Park, F. X. Wu, J. Z. Zhang, T. Hyeon, *J. Am. Chem. Soc.* **2003**, *125*, 6553; b) G. Garnweitner, L. M. Goldenberg, O. V. Sakhno, M. Antonietti, M. Niederberger, J. Stumpe, *Small* **2007**, *3*, 1626.
[8] H. T. Zhang, G. Wu, X. H. Chen, *Mater. Chem. Phys.* **2007**, *101*, 415.
[9] a) T. Taniguchi, N. Sakamoto, T. Watanabe, N. Matsushita, M. Yoshimura, *J. Phys. Chem. C* **2008**, *112*, 4884; b) T. Taniguchi, T. Watanabe, N. Sakamoto, N. Matsushita, M. Yoshimura, *Cryst. Growth Des.* **2008**, *8*, 3725.
[10] J. Kaspar, P. Fornasiero, G. Baiducci, R. Di Monte, N. Hickey, V. Sergo, *Inorg. Chim. Acta* **2003**, *349*, 217.
[11] a) A. Ahniyaz, T. Watanabe, M. Yoshimura, *J. Phys. Chem. B* **2005**, *109*, 6136; b) M. Yashima, H. Arashi, M. Kakihana, M. Yoshimura, *J. Am. Ceram. Soc.* **1994**, *77*, 1067.
[12] a) M. Daturi, E. Finocchio, C. Binet, J.-C. Lavalley, F. Fally, V. Perrichon, H. Vidal, N. Hickey, J. Kaspar, *J. Phys. Chem. B* **2000**, *104*, 9186; b) E. Mamontov, T. Egami, R. Brezny, M. Koranne, S. Tyagi, *J. Phys. Chem. B* **2000**, *104*, 11110.

Received: December 12, 2008
Published Online: April 1, 2009

